[48] M.H. Lee, I. Reynisdottir, J. Massague, Cloning of p57KIP2, a cyclin-dependent kinase inhibitor with unique domain structure and tissue distribution, Genes Dev. 9 (1995) 639–649.
[49] K.S. Smith, S.K. Chanda, M. Lingbeek, D.T. Ross, D. Botstein, M. van Lohuizen, M.L. Cleary, Bmi-1 regulation of INK4A-ARF is a downstream requirement for transformation of hematopoietic progenitors by E2a-Pbx1, Mol. Cell 12 (2003) 393–400.
[50] A.V. Molofsky, R. Pardal, T. Iwashita, I.K. Park, M.F. Clarke, S.J. Morrison, Bmi-1 dependence distinguishes neural stem cell self-renewal from progenitor proliferation, Nature 425 (2003) 962–967.
[51] M. Milyavsky, I. Shats, N. Erez, X. Tang, S. Senderovich, A. Meerson, Y. Tabach, N. Goldfinger, D. Ginsberg, C.C. Harris, V. Rotter, Prolonged culture of telomerase-immortalized human fibroblasts leads to a premalignant phenotype, Cancer Res. 63 (2003) 7147–7157.
[52] K.A. Moore, I.R. Lemischka, "Tie-ing" down the hematopoietic niche, Cell 118 (2004) 139–140.

FEBS 30141 FEBS Letters 579 (2005) 6569–6574

Rat limbal epithelial side population cells exhibit a distinct expression of stem cell markers that are lacking in side population cells from the central cornea

Terumasa Umemoto[a], Masayuki Yamato[a], Kohji Nishida[b], Chinatsu Kohno[a], Joseph Yang[a], Yasuo Tano[b], Teruo Okano[a,*]

[a] *Institute of Advanced Biomedical Engineering and Science, Tokyo Women's Medical University, 8-1 Kawada-cho, Shinjuku-ku, Tokyo 162-8666, Japan*
[b] *Department of Ophthalmology, Osaka University Medical School, Room E7, Yamadaoka 2-2, Suita, Osaka 565-0871, Japan*

Received 14 October 2005; accepted 18 October 2005

Available online 9 November 2005

Edited by Veli-Pekka Lehto

Abstract The side population (SP) phenotype is shared by stem cells in various tissues and species. Here we demonstrate SP cells with Hoechst dye efflux were surprisingly collected from the epithelia of both the rat limbus and central cornea, unlike in human and rabbit eyes. Our results show that rat limbal SP cells have a significantly higher expression of the stem cell markers ABCG2, nestin, and notch 1, compared to central corneal SP cells. Immunohistochemistry also revealed that ABCG2 and the epithelial stem/progenitor cell marker p63 were expressed only in basal limbal epithelial cells. These results demonstrate that ABCG2 expression is closely linked to the stem cell phenotype of SP cells.

Keywords: Corneal epithelium; Limbal epithelium; Stem cell; Side population; ABCG2

1. Introduction

Previous studies using colony forming studies and label-retaining cell assays have suggested that corneal epithelial stem cells reside in the basal layer of the limbal epithelium [1,2], which is located at the transitional zone between the central cornea and the peripheral bulbar conjunctiva. These stem cells are thought to allow for the proper renewal of the corneal epithelium by generating transient amplifying (TA) cells that migrate, proliferate, and differentiate to replace lost or damaged corneal epithelial cells [3–5]. Recently, several researchers, including our group have succeeded in the clinical transplantation of constructs generated from expanded limbal epithelial cells to treat human patients [6–11]. Additionally, because of the highly limited and well characterized localization of corneal epithelial stem cells to the limbus, the corneal epithelial system has been a model system for epithelial stem cell research [12]. However, due to the absence of definite biological markers, the unequivocal identification and isolation of epithelial stem cells within these populations remain elusive.

In 1996, Goodell et al. [13] demonstrated that mouse hematopoietic stem cells with long-term multi-lineage reconstitution abilities could be isolated as a side population (SP) based on their unique ability to efflux the DNA-binding dye Hoechst 33342. Recently, SP cells have also been identified in the hematopoietic compartments of different species [14,15], and have been isolated from various other adult tissues including the liver [16], skeletal muscle [17], brain [18], pancreas [19], and lung [20]. These findings suggest that the SP phenotype represents a common feature of adult tissue-specific stem cells. Zhou et al. [21] reported that the ATP-binding cassette transporter, ABCG2 (also known as BCRP-1 or MXR), is a molecular determinant of this SP phenotype in hematopoietic stem cells. Other studies in a wide range of organs have also indicated that the SP phenotype is largely determined by the expression of ABCG2 [16,19,20,22], a member of the multiple drug resistance (MDR) family of membrane transporters. Taken together, these previous results suggest that the SP phenotype may be an extremely useful tool for the identification of stem cells from various tissues.

Recently, we reported that both the human and rabbit limbal epithelium contains SP cells expressing ABCG2, while SP cells could not be detected in the epithelium of the central cornea [23,24]. In the present study, we investigated the presence of SP cells in both the limbal and corneal epithelium of the rat by fluorescence-activated cell sorting (FACS) and discovered that while cells with the SP phenotype could also be detected in the rat central cornea, only SP cells isolated from the limbal epithelium demonstrated a distinct expression of stem cell markers.

2. Materials and methods

2.1. Cell preparation

Corneoscleral rims were obtained from Wistar rats (8 weeks old, male) and New Zealand white rabbits (2.0 kg, male). Limbal tissues were obtained with scissors, and 2.0 mm-diameter portions of rat corneas and 8.0 mm-diameter portions of rabbit central corneas were obtained by trephination (Fig. 1). Excised tissues from the limbus and central corneas were treated with Dulbecco's modified Eagle's medium (DMEM) containing 120 U/ml dispase II (Godo Shusei, Tokyo, Japan) at 37 °C for 1 h. Epithelial cells were then separated under a dissecting microscope and treated with 0.25% trypsin/1 mM EDTA solution (Invitrogen, Carlsbad, CA) for 20 min at 37 °C, to create single cell suspensions and enzymatic activity was stopped by adding an equal volume of DMEM containing 10% fetal bovine serum (FBS; Moregate BioTech, Queensland, Australia).

*Corresponding author. Fax: +81 3 3359 6046.
E-mail address: tokano@abmes.twmu.ac.jp (T. Okano).

0014-5793/$30.00
doi:10.1016/j.febslet.2005.10.047

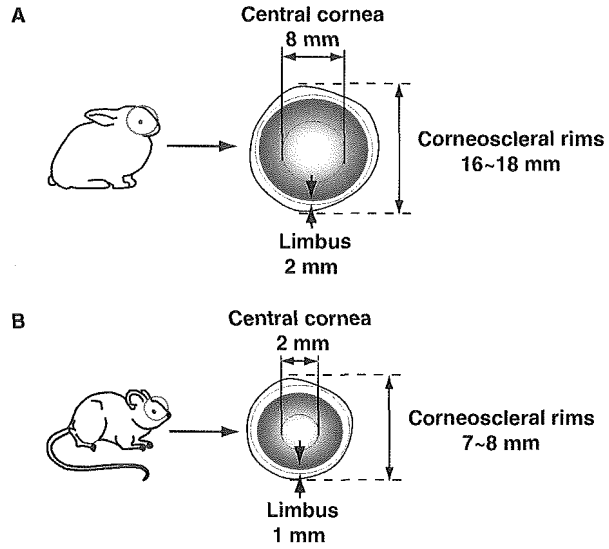

Fig. 1. Isolation of limbal and corneal tissues. (A) Approximately 16–18 mm diameter tissues including cornea, limbus and conjunctiva were isolated from New Zealand white rabbits. From these tissues, 2 mm regions of the limbus were harvested with scissors and 8 mm diameter portions of central corneas were obtained by trephination. (B) In rat tissues, 7–8 mm diameter tissues were isolated and 1 mm limbal tissues and 2 mm diameter portions of central corneas were obtained.

2.2. Hoechst 33342 exclusion assay using fluorescence-activated cell sorting

Single cells isolated from both the limbal epithelium and the corneal epithelium were subjected to FACS using previously described procedures [24].

2.3. Gene expression analysis

Gene expression analyses were conducted using real-time quantitative RT-PCR, as previously described [24].

2.4. Immunohistochemistry

Limbal and corneal tissues were fixed in 10% neutral buffered formalin (Wako Pure Chemicals, Tokyo, Japan) and routinely processed into paraffin-embedded sections. Immunostaining was then performed using the DAKO LSAB kit/HRP (DAB) (Dako Cytomation, Glostrup, Denmark). Briefly, endogenous peroxidase activity was blocked with Peroxidase Blocking Reagent, DAKO S 2001 (Dako). After incubation with 1% bovine serum albumin to block non-specific reactions, sections were incubated with either a 1/200 dilution of anti-ABCG2 antibody (5D3, MBL, Aichi, Japan) or a 1/200 dilution of anti-p63 antibody (4A4, Santa Cruz Biotechnology Inc., Santa Cruz, CA) for 1 h at room temperature, followed by three washes with Dulbecco's phosphate buffered saline (PBS). Sections incubated identically with normal mouse IgG were used as negative controls. After incubation with horseradish peroxidase-conjugated secondary antibodies (Dako) for 30 min at room temperature, the sections were again washed 3 times with PBS. Finally, color development was performed using DAKO ENVISION kit/HRP (DAB) (Dako) and stained sections were visualized using light microscopy.

3. Results

Using FACS, a distinct population of cells with a low Hoechst 33342 blue/red fluorescence was isolated from both rabbit and rat limbal epithelial cells (Fig. 2A and E) analogously to previously reported results for both human and rabbit eyes [23–26], with dye efflux inhibited by treatment with verapamil,

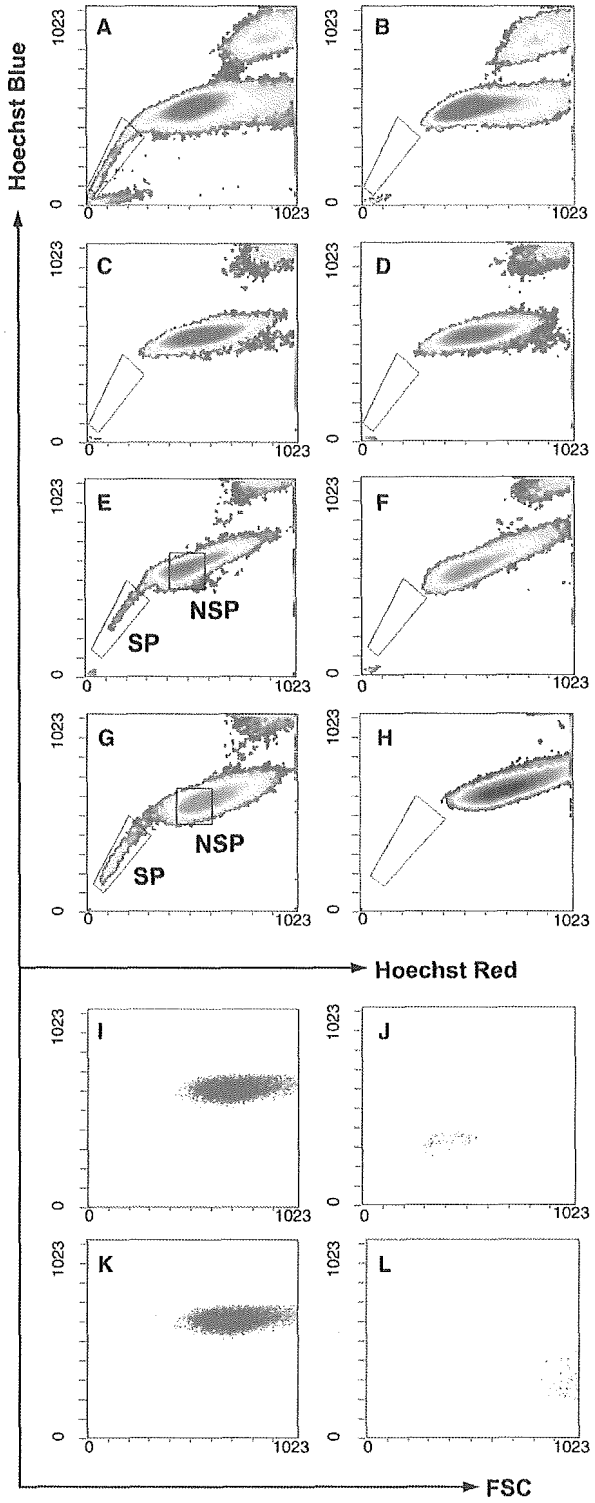

Fig. 2. Hoechst 33342 staining in rabbit and rat limbal and corneal epithelial cells. Epithelial cells were isolated for the cornea and limbus and subjected to Hoechst 33342 exclusion assay. Cells were sorted using FACS and SP cells were detected in the epithelial cells of rabbit limbus (A, B), rabbit cornea (C, D), rat limbus (E, F), and rat cornea (G, H). Dye efflux from SP cells was antagonized by verapamil (B, D, F, H). Forward scattering shows the relative cell size of limbal NSP (I), limbal SP (J), corneal NSP (K) and corneal SP cells (L) in rat. In the density plots of E and G, cells denoted by each enclosed area were regarded as SP and NSP cells for further characterization.

a known inhibitor of Hoechst 33342 dye transport (Fig. 2B and F). The frequency of 0.56% and 0.40% of gated cells for rabbit and rat, respectively, as well as elimination of the SP phenotype by verapamil, was similar to our previously reported results with human eyes [23]. In contrast, cells within the SP gate were barely detected in the corneal epithelium of rabbits (Fig. 2C). However, when epithelial cells from the rat central cornea were subjected to Hoechst 33342 exclusion assays, surprisingly, a significant cell population (4.6% of gated cells) showing the SP phenotype was detected (Fig. 2C). This frequency of rat corneal epithelial SP cells was ten times higher than from the limbal epithelium, but cells showing the SP phenotype were also blocked by treatment with verapamil (Fig. 2H). Forward scatter analyses using FACS also revealed that rat limbal SP cells (Fig. 2J) were smaller in size than both rat limbal NSP cells (Fig. 2I) and rat corneal epithelial NSP cells (Fig. 2K), but that rat corneal epithelial SP cells (Fig. 2L) were much larger than these other cell types.

SP and NSP cells isolated from both the rat limbal epithelium and corneal epithelium were then subjected to real-time quantitative RT-PCR (Fig. 3). Consistent with experimental design, significantly higher expression of ABCG2 mRNA was observed in limbal epithelial SP cells over all other cell fractions (Fig. 3A). In contrast, the expression of ABCG2 could barely be detected in rat corneal epithelial SP cells. These cell fractions were also subjected to gene expression analyses for four common stem cell markers: nestin (Fig. 3B), notch 1 (Fig. 3C), TERT and musashi 1 (data not shown). Significantly higher expression of nestin and notch 1 mRNAs were found in limbal epithelial SP cells compared to limbal epithelial NSP cells as well as both cell fractions isolated from the central corneas. However, gene expression levels of both TERT and musashi 1 were undetectable in all cell fractions (data not shown).

Finally, immunohistochemistry revealed a similar localization of the SP cell marker, ABCG2 with p63, in the rat ocular surface (Fig. 4). p63 is well-known as a marker of epithelial stem and progenitor cells, and p63 positive cells have been previously reported to be localized in the basal layer of the limbal epithelium, but not in the central cornea [27]. Our present results demonstrated that the localization of both ABCG2 and p63 were restricted to the basal layer of the limbal epithelium (Fig. 4C and E), and could not be found in any regions of the central corneas (Fig. 4D and F).

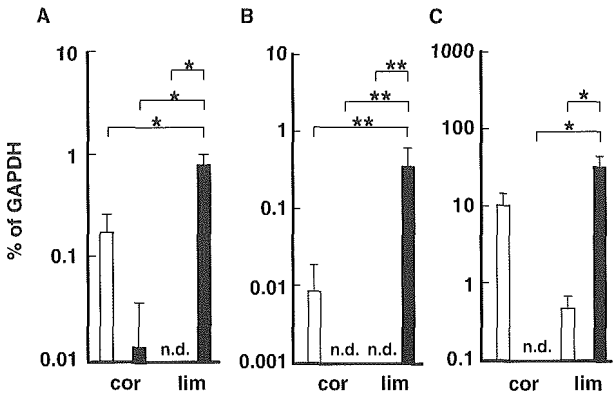

Fig. 3. mRNA analysis of stem cell marker gene expression. Total RNA was extracted from cells isolated by FACS and subjected to real-time quantitative RT-PCR. The relative gene expression of ABCG2 (A), nestin (B), and notch 1 (C) were plotted as a ratio of GAPDH gene expression. Expression levels were detected from NSP cells: gray bars, and SP cells: black bars. Data represent the mean value from three to four independent samples. Error bars indicate the SD ($^{*}P = 0.01$ and $^{**}P < 0.05$, respectively).

4. Discussion

In the present study, we report the isolation of a cell population showing the SP phenotype from rat corneal epithelium and their comparison to SP cells isolated from the limbal epithelium. The SP phenotype is now consistently attributed to various adult tissue-specific stem cells and commonly associated with the functional presence of the ATP-binding cassette transporter, ABCG2 [21,22]. The

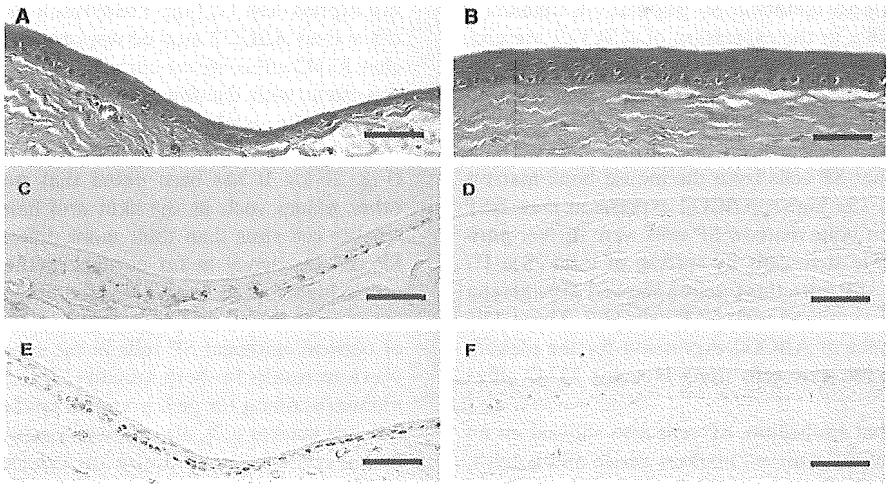

Fig. 4. Immunohistochemistry for ABCG2 and p63 in rat cornea and limbus. The distribution of cells expressing ABCG2 and p63 were examined using immunohistochemistry. Hematoxylin and eosin staining (A, B), and immunostaining with anti-ABCG2 (C, D) and anti-p63 (E, F) antibodies. Left (A, C, E) and right (B, D, F) panels represent rat limbus and cornea, respectively. Scale bars indicate 50 μm.

expression of ABCG2, which is considered a putative marker of the SP phenotype has been reported for cells isolated from numerous tissues, with these cells also exhibiting stem cell-like phenotypes [19,20,22,24]. While our results from FACS have shown that only approximately 0.5% of limbal epithelial cells exhibited the SP cell phenotype regardless of species (Fig. 2A and E) [23,24], immunohistochemistry revealed that a large portion of limbal basal epithelial cells (approximately 10% of total limbal epithelial cells) expressed ABCG2 (Fig. 4C). This apparent discrepancy may be attributed to the transport activity of ABCG2. Limbal basal epithelial cells have relatively little cytoplasmic area, and it is therefore difficult to determine whether ABCG2 molecules were localized to the plasma membranes or in the cytoplasm (Fig. 4C). Since only active ABCG2 transporter present on the cell surface can efflux Hoechst 33342 [20,28], cytoplasmic ABCG2 would be unable to contribute to the observed low Hoechst-derived fluorescence. Additionally, Mogi et al. [28] recently showed that a serine/threonine kinase, Akt, can modulate the SP phenotype by controlling the expression ABCG2, which suggests that ABCG2 function is under strict regulation.

In the present study, while limbal SP cells show higher expression of tissue-specific stem cell markers, in particular ABCG2, compared to the other cell populations examined, these differences in gene expression levels are not as great as observed for both human [23] and rabbit limbal epithelial SP cells [24]. The disparity in the present case is linked to the purity of limbal epithelial SP cells used in the present rat experiments. In the cases of human and rabbit, the central cornea does not contain SP cells that can possibly contaminate the limbal SP population. Additionally, with rat eyes, the significantly smaller size, as well as a lack of the Palisades of Vogt, means that the border between the limbus and central cornea is undefined and difficult to interpret. Therefore, the presence of SP cells in the epithelium of the central cornea inevitably leads to contamination by cells that do not show expression of stem cell markers, causing the relative expression of ABCG2, nestin, and notch 1 to be decreased in the limbal epithelial SP cell fraction that has stem cell-like properties. In contrast to rabbit and human cases, where these factors do not influence the limbal epithelial SP population, differences of approximately 100× in the expression of ABCG2, are considerably greater than the approximately 10× difference observed in the present study, which is a result of this unavoidable contamination. Regarding the relationship between ABCG2 expression and stem cell phenotypes, we have previously shown that SP cells from the mouse bone marrow have approximately 15× higher ABCG2 expression than NSP cells. However, when bone marrow SP cells were further purified for hematopoeitic stem cells by sorting of c-kit$^+$/Sca-1$^+$/Lineage cell marker$^-$ SP cells, this fraction showed 250× greater ABCG2 expression compared with NSP cells [29]. These data suggest the importance of ABCG2 expression for the identification of tissue-specific stem cells using Hoechst 33342 efflux assays.

From the rat limbal epithelium, SP cells also showed an increased expression of the stem cell markers nestin and notch 1, compared to NSP cells from both the limbal epithelium and corneal epithelium, as well as SP cells from the corneal epithelium (Fig. 3). However, even though SP cells were detected in the central cornea, this cell fraction showed significantly lower expression of these stem cell markers compared to limbal epithelial SP cells (Fig. 3).

Nestin is known as a neural stem cell marker [30], but its expression is not limited to neural tissues, and has been recently reported in pancreatic islets [19] and even in the cornea [31]. Specifically in the eyes, retinal SP cells have been reported to exhibit a high expression of nestin mRNA [32]. Notch 1 has also been frequently correlated to a stem cell-like phenotype, by delaying stem cell differentiation via the enhancement of self-renewal in both hematopoietic [33,34] and neural stem cells [35]. The higher expression of notch 1 observed in limbal epithelial SP cells suggests that these cells may indeed resemble other adult stem cells and may indicate a key role of notch 1 signaling in regulating ocular surface homeostasis through well-controlled corneal epithelial turnover. Musashi 1 is another well-recognized neural stem cell marker [36], but its mRNA expression was undetectable in all cell fractions studied, including limbal epithelial SP cells (data not shown), which may imply its specificity to neural tissues. The physiological expression of TERT is highly limited to a very specific number of cell types including proliferating stem cells, reproductive cells, and cancer cells [37,38]. In our experiments, TERT mRNA was not detected in limbal SP cells isolated from normal healthy tissues. Since adult stem cells are considered to be slow-cycling or arrested in the G0/G1 phases of the cell cycle [2,39,40], constitutive expression of TERT is unlikely to be observed in quiescent stem cells. Recent reports have shown that skin epidermal SP cells expressing ABCG2 and putative skin epidermal stem cells exhibiting slow cell cycling are two distinct cell populations [41] and we have also shown that limbal epithelial SP cells with significantly higher expression of ABCG2 represented a quiescent population with stem cell-like properties, without TERT activity [24].

While our results indicate that SP cells isolated from the rat limbal epithelium may constitute a population enriched for stem cells, when SP cells were isolated from rat central corneas, these cells had expression levels of ABCG2 that could be barely detected (Fig. 3A). Immunohistochemistry with anti-ABCG2 antibody also demonstrated that ABCG2 could not be observed in corneal epithelial cells (Fig. 4D). It was recently reported that the human epidermis contains SP cells that do not express ABCG2 [42]. These results imply that a transporter other than ABCG2 may be responsible for the observed Hoechst 33342 efflux in rat corneal epithelial cells. Furthermore, consistent with the absence of ABCG2, rat corneal epithelial SP cells also exhibited similar cell sizes to corneal epithelial NSP cells, and were larger than limbal epithelial SP cells (Fig. 2I–L). It has been noted that stem cells isolated from other tissues such as the skin and hair follicle [43–45] have smaller cell sizes than their more differentiated progeny. The SP cell frequency in rat corneal epithelium (4.6%) was also much higher than in the limbus, as well as results reported for several tissues and organs [13,16,20,23], and the presence of corneal epithelial SP cells in rat eyes were contrary to our previous results for both human [23] and rabbit [24]. Similarly, immunostaining for p63, a known epithelial stem and progenitor cell marker [27], also showed positive staining only in the limbal epithelium and not in the central cornea (Fig. 4E and F). These findings support the theory that even though SP cells were detected in the central corneas of rats, this cell population is distinct from limbal epithelial SP cells and other typical SP cells that show high expression of ABCG2 and are enriched

for tissue-specific stem cells. It is possible that other members of the ABC transporter family may be expressed in corneal epithelial SP cells allowing for the efflux of Hoechst 33342 and therefore the observed SP phenotype, but that these cells lack ABCG2 that is expressed in many tissue-specific stem cells. However, even though it seems likely that corneal epithelial SP cells lack stem cell-like properties, further analysis of the stem cell properties including studies on the capabilities for self-renewal and differentiation are required for a decisive conclusion.

In summary, we have shown that similarly to other species, rat limbal epithelial SP cells show a significantly higher expression of ABCG2 and that these cells also show increased mRNA expression of the stem cell markers nestin and notch 1. However, even with the interesting finding that SP cells may comprise a population enriched for stem cells, the presence of SP cells in the central cornea without ABCG2 expression and seemingly without stem cell-like properties, demonstrates the presence of two distinct SP cell populations in the rat ocular surface. It therefore seems increasingly necessary to confirm the expression of ABCG2 when using SP cells for stem cell research.

Acknowledgments: We appreciate the useful comments and technical criticism of Professor D.W. Grainger (Colorado State University, USA). This work is supported in part by Grants-in-Aid for Scientific Research (16200036 and 16300161), the High-Tech Research Center Program, and the Center of Excellence Program for the 21st Century from the Ministry of Education, Culture, Sports, Science, and Technology in Japan and by the Core Research for Evolution Science and Technology from the Japan Science and Technology Agency.

References

[1] Schermer, A., Galvin, S. and Sun, T.T. (1986) Differentiation-related expression of a major 64K corneal keratin in vivo and in culture suggests limbal location of corneal epithelial stem cells. J. Cell. Biol. 103, 49–62.
[2] Cotsarelis, G., Cheng, S.Z., Dong, G., Sun, T.T. and Lavker, R.M. (1989) Existence of slow-cycling limbal epithelial basal cells that can be preferentially stimulated to proliferate: implications on epithelial stem cells. Cell 57, 201–209.
[3] Kinoshita, S., Friend, J. and Thoft, R.A. (1981) Sex chromatin of donor corneal epithelium in rabbits. Invest. Ophthalmol. Vis. Sci. 21, 434–441.
[4] Thoft, R.A. and Friend, J. (1983) The X, Y, Z hypothesis of corneal epithelial maintenance. Invest. Ophthalmol. Vis. Sci. 24, 1442–1443.
[5] Buck, R.C. (1985) Measurement of centripetal migration of normal corneal epithelial cells in the mouse. Invest. Ophthalmol. Vis. Sci. 26, 1296–1299.
[6] Pellegrini, G., Traverso, C.E., Franzi, A.T., Zingirian, M., Cancedda, R. and De Luca, M. (1997) Long-term restoration of damaged corneal surfaces with autologous cultivated corneal epithelium. Lancet 349, 990–993.
[7] Nishida, K. et al. (2004) Functional bioengineered corneal epithelial sheet grafts from corneal stem cells expanded ex vivo on a temperature-responsive cell culture surface. Transplantation 77, 379–385.
[8] Rama, P., Bonini, S., Lambiase, A., Golisano, O., Paterna, P., De Luca, M. and Pellegrini, G. (2001) Autologous fibrin-cultured limbal stem cells permanently restore the corneal surface of patients with total limbal stem cell deficiency. Transplantation 72, 1478–1485.
[9] Koizumi, N., Inatomi, T., Suzuki, T., Sotozono, C. and Kinoshita, S. (2001) Cultivated corneal epithelial stem cell transplantation in ocular surface disorders. Ophthalmology 108, 1569–1574.
[10] Shimazaki, J., Aiba, M., Goto, E., Kato, N., Shimmura, S. and Tsubota, K. (2002) Transplantation of human limbal epithelium cultivated on amniotic membrane for the treatment of severe ocular surface disorders. Ophthalmology 109, 1285–1290.
[11] Tsai, R.J., Li, L.M. and Chen, J.K. (2000) Reconstruction of damaged corneas by transplantation of autologous limbal epithelial cells. N. Engl. J. Med. 343, 86–93.
[12] Lavker, R.M. and Sun, T.T. (2000) Epidermal stem cells: properties, markers, and location. Proc. Natl. Acad. Sci. USA 97, 13473–13475.
[13] Goodell, M.A., Brose, K., Paradis, G., Conner, A.S. and Mulligan, R.C. (1996) Isolation and functional properties of murine hematopoietic stem cells that are replicating in vivo. J. Exp. Med. 183, 1797–1806.
[14] Goodell, M.A. et al. (1997) Dye efflux studies suggest that hematopoietic stem cells expressing low or undetectable levels of CD34 antigen exist in multiple species. Nat. Med. 3, 1337–1345.
[15] Storms, R.W., Goodell, M.A., Fisher, A., Mulligan, R.C. and Smith, C. (2000) Hoechst dye efflux reveals a novel CD7(+)CD34(−) lymphoid progenitor in human umbilical cord blood. Blood 96, 2125–2133.
[16] Shimano, K. et al. (2003) Hepatic oval cells have the side population phenotype defined by expression of ATP-binding cassette transporter ABCG2/BCRP1. Am. J. Pathol. 163, 3–9.
[17] Jackson, K.A., Mi, T. and Goodell, M.A. (1999) Hematopoietic potential of stem cells isolated from murine skeletal muscle. Proc. Natl. Acad. Sci. USA 96, 14482–14486.
[18] Hulspas, R. and Quesenberry, P.J. (2000) Characterization of neurosphere cell phenotypes by flow cytometry. Cytometry 40, 245–250.
[19] Lechner, A., Leech, C.A., Abraham, E.J., Nolan, A.L. and Habener, J.F. (2002) Nestin-positive progenitor cells derived from adult human pancreatic islets of Langerhans contain side population (SP) cells defined by expression of the ABCG2 (BCRP1) ATP-binding cassette transporter. Biochem. Biophys. Res. Commun. 293, 670–674.
[20] Summer, R., Kotton, D.N., Sun, X., Ma, B., Fitzsimmons, K. and Fine, A. (2003) Side population cells and Bcrp1 expression in lung. Am. J. Physiol. Lung. Cell. Mol. Physiol. 285, L97–L104.
[21] Zhou, S. et al. (2001) The ABC transporter Bcrp1/ABCG2 is expressed in a wide variety of stem cells and is a molecular determinant of the side-population phenotype. Nat. Med. 7, 1028–1034.
[22] Bunting, K.D. (2002) ABC transporters as phenotypic markers and functional regulators of stem cells. Stem Cells 20, 11–20.
[23] Watanabe, K. et al. (2004) Human limbal epithelium contains side population cells expressing the ATP-binding cassette transporter ABCG2. FEBS Lett. 565, 6–10.
[24] Umemoto, T., Yamato, M., Nishida, K., Yang, J., Tano, Y. and Okano, T. (in press). Limbal epithelial side population cells have stem cell-like properties, including quiescent state. Stem Cells.
[25] Budak, M.T., Alpdogan, O.S., Zhou, M., Lavker, R.M., Akinci, M.A. and Wolosin, J.M. (2005) Ocular surface epithelia contain ABCG2-dependent side population cells exhibiting features associated with stem cells. J. Cell. Sci. 118, 1715–1724.
[26] de Paiva, C.S., Chen, Z., Corrales, R.M., Pflugfelder, S.C. and Li, D.Q. (2005) ABCG2 transporter identifies a population of clonogenic human limbal epithelial cells. Stem Cells 23, 63–73.
[27] Pellegrini, G. et al. (2001) p63 Identifies keratinocyte stem cells. Proc. Natl. Acad. Sci. USA 98, 3156–3161.
[28] Mogi, M. et al. (2003) Akt signaling regulates side population cell phenotype via Bcrp1 translocation. J. Biol. Chem. 278, 39068–39075.
[29] Umemoto, T., Yamato, M., Nishida, K., Yang, J., Tano, Y. and Okano, T. (2005) p57(Kip2) is expressed in quiescent mouse bone marrow side population cells. Biochem. Biophys. Res. Commun. 337, 14–21.
[30] Lendahl, U., Zimmerman, L.B. and McKay, R.D. (1990) CNS stem cells express a new class of intermediate filament protein. Cell 60, 585–595.
[31] Seigel, G.M., Sun, W., Salvi, R., Campbell, L.M., Sullivan, S. and Reidy, J.J. (2003) Human corneal stem cells display functional neuronal properties. Mol. Vis. 9, 159–163.
[32] Bhattacharya, S., Jackson, J.D., Das, A.V., Thoreson, W.B., Kuszynski, C., James, J., Joshi, S. and Ahmad, I. (2003) Direct identification and enrichment of retinal stem cells/progenitors by

Hoechst dye efflux assay. Invest. Ophthalmol. Vis. Sci. 44, 2764–2773.
[33] Kumano, K. et al. (2001) Notch1 inhibits differentiation of hematopoietic cells by sustaining GATA-2 expression. Blood 98, 3283–3289.
[34] Stier, S., Cheng, T., Dombkowski, D., Carlesso, N. and Scadden, D.T. (2002) Notch1 activation increases hematopoietic stem cell self-renewal in vivo and favors lymphoid over myeloid lineage outcome. Blood 99, 2369–2378.
[35] Chojnacki, A., Shimazaki, T., Gregg, C., Weinmaster, G. and Weiss, S. (2003) Glycoprotein 130 signaling regulates Notch1 expression and activation in the self-renewal of mammalian forebrain neural stem cells. J. Neurosci. 23, 1730–1741.
[36] Sakakibara, S. et al. (1996) Mouse-Musashi-1, a neural RNA-binding protein highly enriched in the mammalian CNS stem cell. Dev. Biol. 176, 230–242.
[37] Belair, C.D., Yeager, T.R., Lopez, P.M. and Reznikoff, C.A. (1997) Telomerase activity: a biomarker of cell proliferation, not malignant transformation. Proc. Natl. Acad. Sci. USA 94, 13677–13682.
[38] Meeker, A.K. and Coffey, D.S. (1997) Telomerase: a promising marker of biological immortality of germ, stem, and cancer cells. A review. Biochemistry (Mosc). 62, 1323–1331.
[39] Cotsarelis, G., Sun, T.T. and Lavker, R.M. (1990) Label-retaining cells reside in the bulge area of pilosebaceous unit: implications for follicular stem cells, hair cycle, and skin carcinogenesis. Cell 61, 1329–1337.
[40] Bickenbach, J.R. and Chism, E. (1998) Selection and extended growth of murine epidermal stem cells in culture. Exp. Cell. Res. 244, 184–195.
[41] Triel, C., Vestergaard, M.E., Bolund, L., Jensen, T.G. and Jensen, U.B. (2004) Side population cells in human and mouse epidermis lack stem cell characteristics. Exp. Cell. Res. 295, 79–90.
[42] Terunuma, A., Jackson, K.L., Kapoor, V., Telford, W.G. and Vogel, J.C. (2003) Side population keratinocytes resembling bone marrow side population stem cells are distinct from label-retaining keratinocyte stem cells. J. Invest. Dermatol. 121, 1095–1103.
[43] Li, A., Simmons, P.J. and Kaur, P. (1998) Identification and isolation of candidate human keratinocyte stem cells based on cell surface phenotype. Proc. Natl. Acad. Sci. USA 95, 3902–3907.
[44] Tani, H., Morris, R.J. and Kaur, P. (2000) Enrichment for murine keratinocyte stem cells based on cell surface phenotype. Proc. Natl. Acad. Sci. USA 97, 10960–10965.
[45] Kim, D.S., Cho, H.J., Choi, H.R., Kwon, S.B. and Park, K.C. (2004) Isolation of human epidermal stem cells by adherence and the reconstruction of skin equivalents. Cell. Mol. Life Sci. 61, 2774–2781.

STEM CELLS®
Tissue-Specific Stem Cells

Limbal Epithelial Side-Population Cells Have Stem Cell–Like Properties, Including Quiescent State

TERUMASA UMEMOTO,[a] MASAYUKI YAMATO,[a] KOHJI NISHIDA,[b] JOSEPH YANG,[a] YASUO TANO,[b] TERUO OKANO[a]

[a]Institute of Advanced Biomedical Engineering and Science, Tokyo Women's Medical University, Tokyo, Japan; [b]Department of Ophthalmology, Osaka University Medical School, Osaka, Japan

Key Words. Side population • Quiescence • ABCG2 • Limbal epithelium • Corneal epithelium

ABSTRACT

Corneal epithelial (CE) stem cells are believed to reside in the basal layer of the limbal epithelium but remain poorly understood due to the lack of an accepted in vivo reconstitution assay as well as definitive markers for epithelial stem cells. It has been reported that side-population (SP) cells with the ability to efflux the DNA-binding dye Hoechst 33342 have stem cell–like properties and that the SP phenotype accurately represents a quiescent and immature stem cell population in the adult bone marrow. In the present study, we investigated whether SP cells isolated from the limbal epithelium have stem cell–like properties. SP cells, separated by fluorescence-activated cell sorting, comprise approximately 0.4% of all limbal epithelial cells and have markedly higher expression of the stem cell markers ABCG2, Bmi-1, and nestin but no expression of markers for differentiated CE cells compared with non-SP cells. Cell-cycle and telomerase activity analyses revealed that SP cells are growth arrested and reside in the quiescent state. Moreover, limbal epithelial SP cells did not demonstrate proliferative capabilities under typical in vitro epithelial cell culture conditions using 3T3 feeder layers. These findings present the possibility that quiescent limbal epithelial SP cells may represent an extremely immature stem cell population compared with currently defined epithelial stem or progenitor cells. STEM CELLS *2006;24:86–94*

INTRODUCTION

Adult tissue-specific stem cells have the unique ability for self-renewal and govern the maintenance of their tissue of origin. These stem cells, which reside in specialized niches, are vital in sustaining long-term repopulation of the specific tissue via progression through a series of increasingly differentiated cells. Adult stem cells are particularly resistant to various stresses, and the proper regulation of the stem cell niche is required in maintaining their immature, undifferentiated form. Of all adult lineages, hematopoietic stem cells (HSCs) are the most well-established, as there is significant knowledge and insight into the factors and characteristics that are necessary for the regulation of their self-renewal and differentiation. HSCs previously have been shown to be both quiescent and antiapoptotic, meeting the criteria for tissue-specific adult stem cells [1]. This noncycling state is believed to protect HSCs from external stresses and allows for the maintenance of their self-renewal. It has recently been demonstrated that the single characteristic that

Correspondence: Professor Teruo Okano, Ph.D., Institute of Advanced Biomedical Engineering and Science, Tokyo Women's Medical University, 8-1 Kawada-cho, Shinjuku-ku, Tokyo 162-8666, Japan. Telephone: 81-3-3353-8111, ext. 30233; Fax: 81-3-3359-6046; e-mail: tokano@abmes.twmu.ac.jp Received February 17, 2005; accepted for publication July 1, 2005; available online without subscription through the open access option. 1066-5099/2006/$12.00/0 doi: 10.1634/stemcells.2005-0064

most accurately represents quiescent HSCs is the side-population (SP) phenotype [1, 2]. SP cells have the unique ability to efflux the DNA-binding dye Hoechst 33342 via the ATP-binding cassette transporter G2 (ABCG2), a member of the multiple-drug resistance family of membrane transporters [3–6]. Bone marrow SP cells have the capability for the long-term multilineage reconstitution of the hematopoietic system [2, 7], and it is believed that these SP cells represent quiescent HSCs more accurately than HSCs characterized by other means. In addition, SP cells have been isolated from various other adult tissues, including liver [8, 9], skeletal muscle [10], and lung [11], demonstrating that this phenotype with the existence of ABCG2 and the ability to efflux Hoechst 33342 may represent a common feature of all adult stem cells.

Corneal epithelial (CE) stem cells are thought to reside in the basal layer of the limbus [12, 13], the transitional zone between the cornea and the peripheral bulbar conjunctiva. CE stem cells maintain the ocular surface by generating transient amplifying (TA) cells that migrate, proliferate, and differentiate to replace lost or damaged CE cells [14–16]. Whereas traditional methods use colony-forming assays or pulse-chase experiments of labeled thymidine, the lack of both definitive markers and an established in vivo reconstitution assay still remain serious obstacles in the unequivocal identification of not only CE stem cells but also other epithelial stem cells. Recently we have demonstrated that the limbal epithelium contains SP cells that express ABCG2 [17]. It is believed that these cells may allow for the separation of CE stem cells from their more differentiated progeny. We therefore investigated the properties of limbal epithelial SP cells to determine whether they possess stem cell–like properties. Our results demonstrate that limbal epithelial SP cells closely resemble HSCs and strongly suggest that these cells allow for the first insights into a true epithelial stem cell population.

Materials and Methods

Cell Preparation

Corneoscleral rims were obtained from New Zealand white rabbits. Limbal tissues were obtained with scissors, and 2.0-mm-diameter portions of the central corneas were obtained by trephination. Excised tissues from the limbus and central corneas were treated with Dulbecco's modified Eagle's medium (DMEM) containing 250 U/ml dispase II (Godo Shusei, Tokyo, Japan, http://www.godo.jp) at 37°C for 1 hour. Epithelial cells were then separated under a dissecting microscope and treated with 0.25% trypsin/1 mM EDTA solution (Invitrogen, Carlsbad, CA, http://www.invitrogen.com) for 20 minutes at 37°C to create single-cell suspensions from the limbal epithelium and corneal epithelium, and enzymatic activity was stopped by adding an equal volume of DMEM containing 10% fetal bovine serum (FBS) (Moregate BioTech, Queensland, Australia, http://www.moregatebiotech.com).

Hoechst 33342 Exclusion Assay Using Fluorescence-Activated Cell Sorting

Limbal epithelial and CE cells were resuspended at a concentration of 10^6 cells/ml in staining medium (DMEM containing 2% FBS and 10 mM HEPES). Cell suspensions were incubated in staining medium containing 3 μg/ml Hoechst 33342 (Sigma, St. Louis, http://www.sigmaaldrich.com) for 90 minutes at 37°C. For inhibition experiments, 50 μM of either R(+)-verapamil (Sigma) or tryprostatin-A (Alexis Biochemicals, Carlsbad, CA, http://www.alexis-corp.com) was added to the staining medium 30 minutes before the addition of Hoechst 33342. After staining, cells were washed two times with Dulbecco's phosphate-buffered saline (PBS) containing 2% FBS and 1 mM HEPES and then resuspended. Before analysis and cell sorting, propidium iodide (Sigma) was added at a final concentration of 2 μg/ml to distinguish between live and nonviable cells. Analysis and cell sorting were performed using a dual-laser fluorescence-activated cell sorter (FACS) (EPICS® ALTRA FACS analysis system, Beckman Coulter, Fullerton, CA, http://www.beckmancoulter.com). Hoechst 33342 was excited at 350 nm using a UV laser, and fluorescence emission was detected through 450-nm band-pass (BP) (Hoechst blue) and 675-nm long-pass (Hoechst red) filters, respectively. Propidium iodide was excited at 488 nm (argon ion laser), and fluorescence emission was detected through a 610-nm BP filter.

Gene Expression Analysis

After sorting and isolation of SP and non-SP (NSP) cells from the limbal epithelium and viable CE cells from central corneas, total RNA was obtained from 10,000 SP, NSP, and CE cells using ISOGEN (Nippon Gene, Tokyo, Japan, http://www.nippongene.com) according to the manufacturer's suggested protocol. After treatment with DNase I (Nippon Gene), single-stranded cDNA was created with the Superscript First-Strand System for reverse transcription–polymerase chain reaction (RT-PCR) (Invitrogen) and used as PCR templates. Primer pairs and TaqMan MGB probes labeled with 6-carboxyfluorescein (FAM) at the 5′-end and nonfluorescent quencher at the 3′-end were designed with Assay-by-Design (Applied Biosystems, Foster City, CA, http://www.appliedbiosystems.com). Quantitative PCR was performed with an iCycler iQTM Real-Time Detection System (Bio-Rad, Hercules, CA, http://www.bio-rad.com). Thermocycling programs consisted of an initial cycle at 50°C for 2 minutes and 95°C for 10 minutes, followed by 50 cycles of 95°C for 15 seconds and 60°C for 1 minute. Negative con-

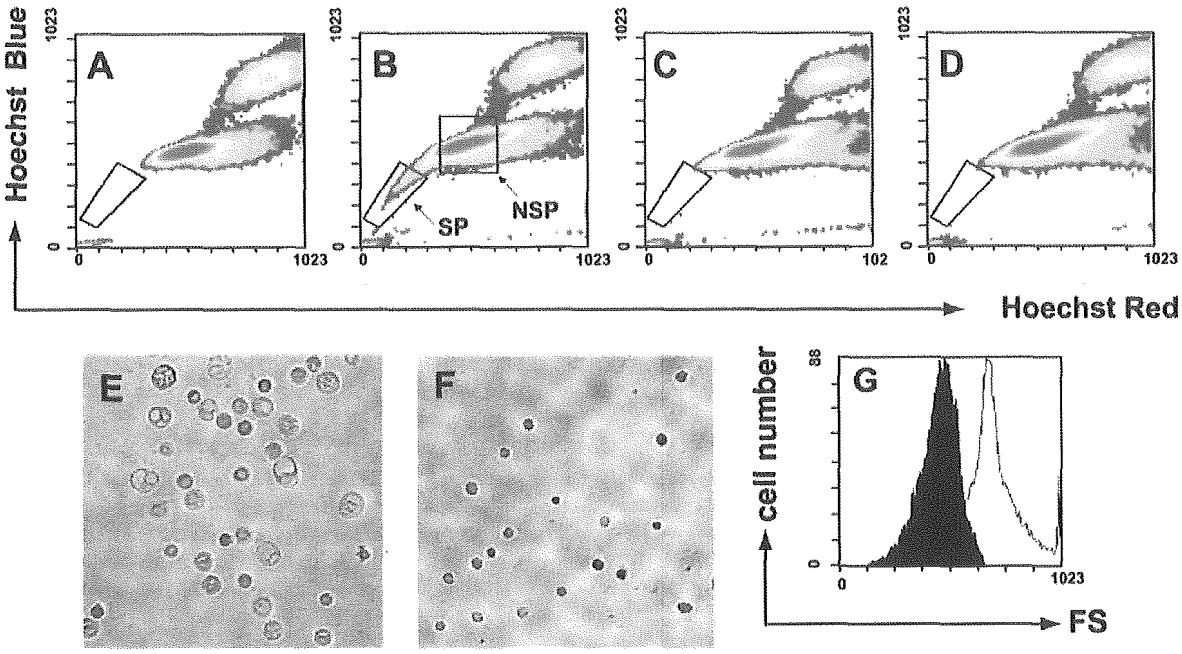

Figure 1. Hoechst 33342 staining in rabbit limbal and corneal epithelial cells. Epithelial cells were removed from the limbus and cornea and analyzed for Hoechst 33342 efflux by fluorescence-activated cell sorting (FACS). Side-population (SP) cells were detected in epithelial cells after Hoechst 33342 staining from the cornea **(A)** and the limbus **(B)**. In the density plot of **(B)**, the cells denoted by each enclosed area were regarded as SP cells or non-SP (NSP) cells for further characterization. Limbal epithelial cells were pretreated with each transporter inhibitor, verapamil, an inhibitor of MDR **(C)**, or tryprostatin-A (TPS-A), a specific inhibitor of ABCG2 **(D)**, before staining with Hoechst 33342. After isolation, NSP cells **(E)** and SP cells **(F)** were centrifuged onto glass slide slips and observed with a phase-contrast microscope (magnification ×100). Forward scatter (FS) by FACS was analyzed in SP (black) and NSP (white) cells to examine cell size in each fraction **(G)**.

trols using non–reverse transcribed total RNA as template strands were performed for all experiments. All assays were run in duplicate for more than four individual samples. mRNA expression levels were normalized with the expression level of glyceraldehyde-3-phosphate dehydrogenase (GAPDH). To represent expression levels of individual mRNAs, we used an mRNA expression index that divided the value of the specific gene copies by the value for GAPDH. To compare mRNA expression between SP and NSP cells, the Mann-Whitney rank-sum test was applied and statistics were calculated using SigmaStat 2.0 (SPSS, Chicago, IL, http://www.spss.com).

Colony-Forming Assay

Feeder layers were prepared by seeding of mitomycin C–treated NIH-3T3 cells at a density of 2 × 104 cells/cm^2, and SP, NSP, or all viable limbal epithelial cells were seeded at a density of 1,000 cells per 60-mm dish (Becton, Dickinson and Company, Franklin Lakes, NJ, http://www.bd.com). After culture for approximately 10 days at 37°C, colonies were fixed with 10% formalin (Wako Chemicals, Osaka, Japan, http://www.wako-chem.co.jp/english) and stained with 2% rhodamine B (Sigma), and the entire dish surfaces were scanned under a dissecting microscope.

Cell-Cycle Analysis

Limbal epithelial SP cells and total limbal epithelial cells were pelleted by centrifugation and resuspended in a solution containing 4 mM sodium citrate (pH 7.6), 0.2% Nonidet P-40, and 50 μg/ml propidium iodide. After incubation on ice for 30 minutes, cell suspensions were treated with 0.25 mg/ml RNase A for 15 minutes at 37°C to remove double-stranded RNA. Cells were finally analyzed by flow cytometry at an excitation wavelength of 488 nm.

Telomerase Activity

Using the TRAPeze XL telomerase Detection Kit (Chemicon, Temecula, CA, http://www.chemicon.com), telomerase activity was investigated in SP, NSP, and corneal epithelial cells according to the manufacturer's suggested protocol. Briefly, 10,000 SP, NSP, or CE cells were pelleted by centrifugation and resuspended in CHAPS XL lysis buffer. The reaction mixtures containing the cell lysates were then incubated for 60 minutes at 37°C and subjected to PCR. PCR consisted of 30 cycles at 94°C for 30 seconds, 56°C for 30 seconds, and 72°C for 1 minute. Reaction mixtures were then subjected to electrophoresis on a 10% polyacrylamide gel. After electrophoresis, the gel was stained with SYBR Green I

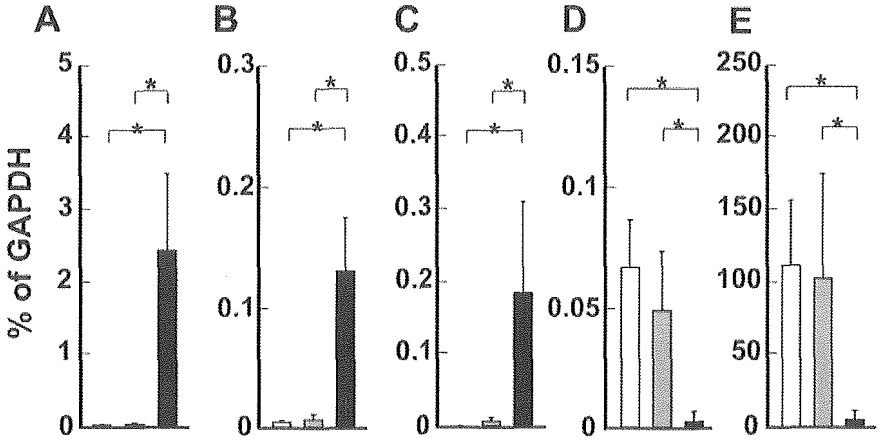

Figure 2. Quantification of mRNA in limbal epithelial side-population (SP) and non-SP (NSP) cells and corneal epithelial (CE) cells. Total RNA was extracted from limbal epithelial SP cells, NSP cells, and CE cells after fluorescence-activated cell sorting and subjected to real-time quantitative reverse transcription–polymerase chain reaction. Relative expression of the selected genes was normalized to that of GAPDH for each sample. mRNA expression of ABCG2 **(A)**, Bmi-1 **(B)**, nestin **(C)**, CK 3 **(D)**, and CK 12 **(E)** is shown. Expression levels were determined from SP cells (black bar), NSP cells (gray bar), and CE cells (white bar) for each individual mRNA. Data represent the mean value from four to six samples. Error bars indicate the standard deviation (*$p < .01$).

(Molecular Probes, Eugene, OR, http://probes.invitrogen.com) and the image was recorded with Typhoon (Amersham Biosciences, Piscataway, NJ, http://www.amersham.com).

Results

Limbal Epithelium Contains a Side Population with Cells of Smaller Size

To determine whether SP cells were present in either the limbal or corneal epithelium, both epithelial cell types were isolated from the eyes of New Zealand white rabbits and subjected to Hoechst 33342 dye efflux assay. SP cells were nearly undetected in corneal epithelial cells (Fig. 1A; 0.01% gated cells), similar to results in human eyes [17]. In contrast, a distinct population with decreased Hoechst 33342 blue/red fluorescence was detected in limbal epithelial cells (Fig. 1B; 0.40% gated cells), also similar to previous results with human limbus [17]. Hoechst 33342 efflux was antagonized by both verapamil, an inhibitor of Hoechst 33342 dye transport, and tryprostatin A, a specific inhibitor of ABCG2 (Figs. 1C, 1D) in the same fashion as previous results using different tissues of origin [8, 11, 18, 19]. SP and NSP cell fractions were collected by cell sorting as denoted in Figure 1B, and microscopic analysis (Figs. 1E, 1F) revealed that SP cells had a smaller cell size compared with NSP cells. These results were also confirmed by forward scatter analysis using FACS (Fig. 1G).

Limbal Epithelial SP Cells Express Stem Cell–Related Genes

To examine whether SP cells have stem cell–like phenotypes, gene expression analyses of SP and NSP cells from the limbus

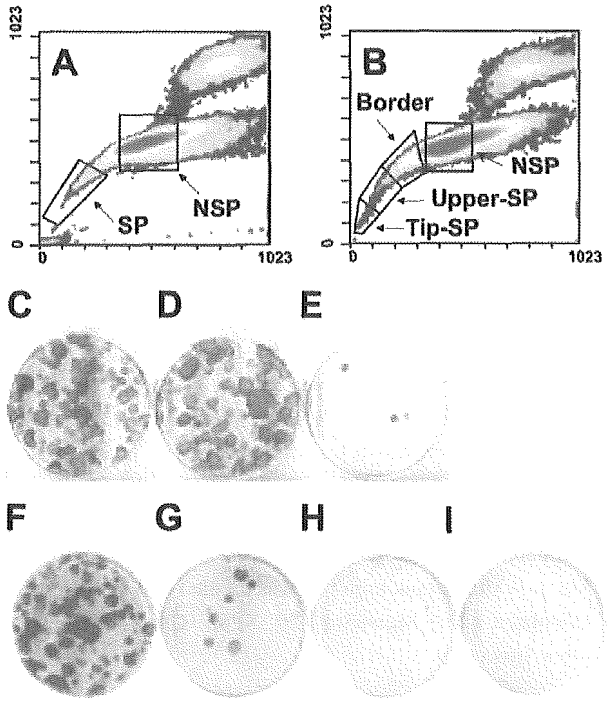

Figure 3. Colony-forming assay with limbal epithelial side-population (SP) cells and non-SP (NSP) cells. Limbal epithelial cells were separated by fluorescence-activated cell sorting into SP and NSP cells **(A)** for colony-forming assays. For in-depth analysis, limbal epithelial cells were sorted into four gates: Tip-SP, upper-SP, border, and NSP cells **(B)**. After cell sorting, viable limbal epithelial cells **(C)**, NSP cells **(D)**, or SP cells **(E)** were seeded onto mitomycin C–treated NIH-3T3 feeder layers at a density of 1,000 cells per 60-mm dish. For detailed studies, NSP cells **(F)**, border cells **(G)**, upper-SP cells **(H)**, or Tip-SP cells **(I)** were subjected to colony-forming assays under the same conditions. Cells were cultured for approximately 10 days followed by fixation and staining with rhodamine B.

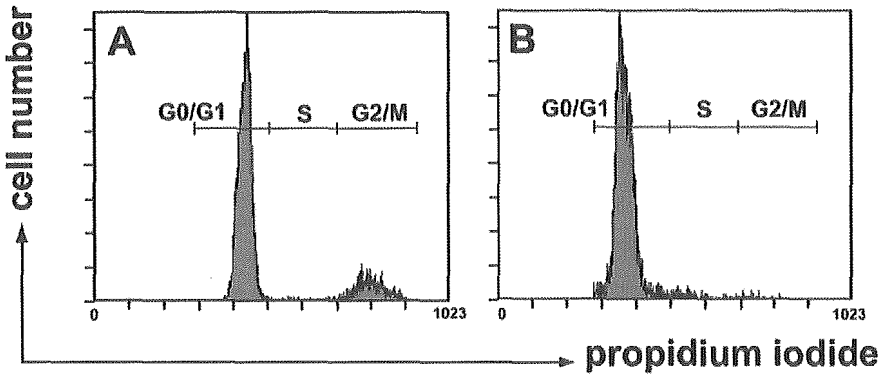

Figure 4. Cell-cycle state of limbal epithelial side-population (SP) cells. After sorting of all viable limbal epithelial cells and SP cells, cell membranes were disrupted using Nonidet P-40 followed by staining with propidium iodide. The cell-cycle phase in which each individual cell resided, from either all viable limbal epithelial cells **(A)** or SP cells **(B)**, was detected by flow cytometry.

as well as CE cells were conducted using real-time quantitative RT-PCR. ABCG2, which is required to induce the SP phenotype; Bmi-1, necessary for the self-renewal of HSCs and neural stem cells [20–24]; and nestin, an intermediate filament specifically expressed in neural stem cells [25] were used as stem cell markers. Significant expression of ABCG2, Bmi-1, and nestin was detected in SP cells, but neither NSP cells nor CE cells showed expression of these genes. On the contrary, cytokeratin 3 (CK3) and cytokeratin 12 (CK12), which are known markers of differentiated CE cells [26], were significantly expressed in both NSP and CE cells but not in SP cells (Fig. 2). Additionally, results from immunostaining with anti-ABCG2 antibodies have previously revealed that ABCG2-positive cells comprise only a small portion of the human limbal epithelium, with negative staining in central corneas [17, 27].

SP Cells Are Growth Arrested in the Quiescent State

Because SP cells corresponded to a CE stem cell phenotype in location and gene expression, we investigated whether SP cells (Fig. 3A) have a strong capacity for proliferation using colony-forming assays. Unexpectedly, whereas cell fractions of all limbal epithelial cells (Fig. 3C) or NSP cells (Fig. 3D) had high proliferative capabilities, SP cells (Fig. 3E) demonstrated an extremely low colony-forming efficiency (CFE) (Table 1). Even when culture conditions were modified, such as the addition of various cytokines and growth factors, coculture with NSP cells, or isolation from wounded corneas, SP cells were still unable to form a significant number of colonies in vitro (data not shown). These results suggested that SP cells have almost no capacity for proliferation under normal in vitro culture conditions for CE cells.

To investigate the proliferative potential of limbal SP cells in greater detail, limbal epithelial cells were sorted into four gates, representing the tip-SP, upper-SP, border, and NSP cells (Fig. 3B). Results from colony-forming assays showed that whereas NSP cells (Fig. 3F) had a CFE comparable to all limbal epithelial cells, border (Fig. 3G), upper-SP (Fig. 3H), and tip-SP (Fig. 3I) cells all had negligible CFEs compared with NSP cells (Table 1). Therefore, the colony-forming ability of limbal epithelial cells is likely nearly completely derived from the NSP cell fraction.

Because SP cells demonstrated almost no proliferative capabilities in vitro, we investigated the cell-cycle state of SP cells. After sorting of SP cells and viable limbal epithelial cells, each cell fraction was permeabilized and stained with propidium iodide, followed by flow cytometric analysis. Although the cell cycle of limbal epithelial cells was promoted with active cell division, SP cells were nearly all growth arrested in G0/G1 (Fig. 4, Table 2).

Results from colony-forming assays (Fig. 3, Table 1) and cell-cycle analysis (Fig. 4, Table 2) suggested that SP cells may represent a quiescent stem cell population. To confirm this possibility, we examined telomerase activity in SP cells using

Table 1. Colony-forming efficiencies and detailed analysis of limbal epithelial cells subjected to Hoechst 33342 exclusion assays

	Viable cells (%)	CFE (%)
All	—	8.49 ± 3.03
NSP	66.1 ± 3.92	7.75 ± 2.42
SP	0.40 ± 0.19	0.38 ± 0.09
Border	2.83 ± 0.55	0.83 ± 0.15
Upper SP	0.20 ± 0.04	0.10 ± 0.10
Tip SP	0.03 ± 0.01	ND

Epithelial cells subjected to fluorescence-activated cell sorting were sorted, and the corresponding percentages of cells in each gate from Figures 3A and 3B are presented. Additionally, colony-forming efficiencies for cells from each gate are shown. Values are presented as means ± standard deviations.
Abbreviations: CFE, colony-forming efficiency; ND, not determined.

Table 2. Cell-cycle state of limbal epithelial side-population cells

	G0/G1	S	G2/M
SP	96.9 ± 0.6	1.1 ± 0.3	1.6 ± 0.4
All	78.6 ± 2.5	3.2 ± 0.8	18.4 ± 1.7

Values correspond to the percentage of cells in each cell-cycle phase. Values are presented as means ± standard deviations.

the TRAP assay. It has been previously reported that quiescent stem cells have no telomerase activity but that it is upregulated in actively proliferating TA and progenitor cells in hair follicles [28], skin [29], and bone marrow [30]. Cell lysates from each cell fraction purified by FACS were reacted to lengthen telomeres, followed by amplification of the product with PCR. HeLa cells were used as a positive control, and each cell fraction was also treated with heat as a negative control. We found that both SP and CE cells had no telomerase activity, whereas NSP cells demonstrated weak activity (Fig. 5).

Discussion

Limbal Epithelial SP Cells Resemble Other Adult Tissue-Specific Stem Cells

In the present study, we demonstrated that limbal epithelial SP cells have HSC-like properties, including small size, increased expression of the stem cell markers ABCG2, Bmi-1, and nestin, and an SP phenotype. Immature cell types such as stem cells are thought to be much smaller in size compared with normal cells, and limbal epithelial SP cells were significantly smaller than NSP cells and appeared more immature and simple in cell shape, thus supporting the view that SP cells represent a CE stem cell population or, at the very least, an extremely immature cell population.

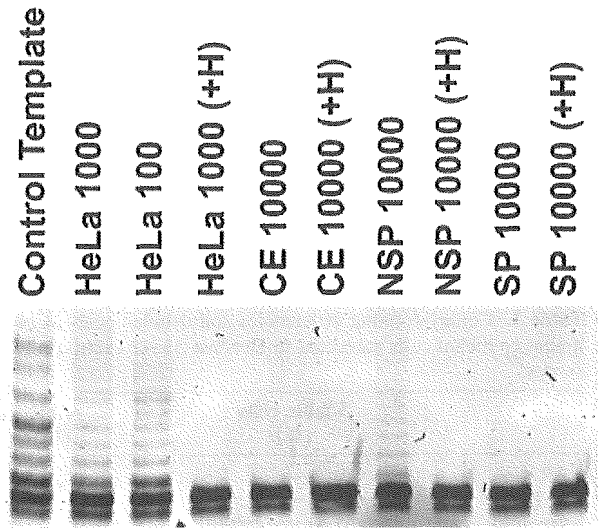

Figure 5. Telomerase activity. After cell sorting, telomerase activity was examined by the telomeric repeat amplifying protocol (TRAP) assay for each cell fraction. A control template, containing several telomeric repeats, was used at a concentration of 0.2 mol/μl. HeLa cells were selected as a positive control. Each cell lysate was also treated with heat (+H) as a negative control. After TRAP assay, each reaction mixture was subjected to polyacrylamide electrophoresis followed by staining with SYBR green I. The number of cells used for each sample is shown. Abbreviations: CE, corneal epithelial; NSP, non–side population; SP, side population.

For the SP phenotype to be indicative of stem cell–like properties, the expression of ABCG2 is required [7, 31, 32]. Because adult stem cells are known to be particularly resistant to various stresses, the expression of ABCG2 likely acts as a protective mechanism, allowing for the efflux of various soluble factors or toxins that could result in the premature differentiation of SP cells.

Bmi-1, a member of the polycomb gene family, is expressed not only in HSCs but also in neural stem cells and is vital to the self-renewal of adult stem cells [20–24]. The increased expression of Bmi-1 in limbal epithelial SP cells therefore also seems likely to be critically involved in the self-renewal of CE stem cells. Bmi-1 decreases expression of p16 and p19 [20, 21, 33], known cyclin-dependent kinase inhibitors, and increases telomerase activity [34]. However, even though Bmi-1 is believed to promote increased proliferation of cells, higher expression of Bmi-1 has been correlated with the maintenance of the stem cell phenotype. It seems that adult stem cells have high proliferative potential, but other regulatory factors act to prevent unnecessary proliferation and carefully regulate the generation of differentiated progeny.

Nestin, an intermediate filament protein and known neural stem cell marker [25], was also more highly expressed in SP cells compared with other cell fractions. Increased nestin expression has previously been detected in SP cells isolated from other tissues, such as the pancreas [19] and retina [18], and may therefore be a characteristic cytoskeletal molecule of not only neural stem cells but also other adult stem cells with the SP phenotype.

Therefore, the previously proposed environment of the basal layer, being the most isolated from the exposed ocular surface, in conjunction with the expression of the stem cell markers ABCG2, Bmi-1, and nestin, may allow for the proper maintenance and self-renewal of limbal epithelial SP cells.

SP Cells Likely Represent a Quiescent Stem Cell Population in the Limbal Epithelium

In the present study, most limbal epithelial SP cells were found to be growth arrested in G0/G1, compared with all cells isolated from the limbal epithelium. HSCs are known to be quiescent in the bone marrow niche [1, 35], and limbal epithelial SP cells therefore also resemble HSCs by being cell-cycle arrested. The

quiescent state of limbal epithelial SP cells led to the interesting finding that SP cells did not proliferate and could not create colonies in vitro, like previously defined epithelial stem cells. Whereas tip-SP cells revealed no colony formation, very low CFEs were observed for the SP, upper-SP, and border-gated cells (Table 1). These values, however, seem correlated with the purity of the SP fraction after cell sorting, because SP cells isolated by FACS inevitably contain approximately 1%–2% contamination by other cells (data not shown). Therefore, it is believed that the observed CFE is likely due to contamination by NSP cells, which account for the proliferative capabilities of all cells in the limbal epithelium. Moreover, SP cells showed lower expression of $\alpha 6$ and $\beta 1$ integrins (data not shown), which are known to be highly expressed in cells with strong proliferative capabilities [36–38].

Although a recent study reported that limbal epithelial SP cells had the ability to form colonies [39], their experimental procedures had several different conditions. In particular, the seeded cell density, UV laser intensity used for FACS, and primary cell culture before cell sorting were most likely the cause for the conflicting results. In their colony-forming assay, epithelial cells were seeded at a density that was 20 times higher than in the present study. Therefore, even though scanned images revealed dish surfaces that were nearly completely covered by proliferating cells, results actually showed significantly lower CFEs (4% for SP and 1% for NSP cells) compared with our present results (approximately 10% for NSP cells). Although these differences may be due to culture conditions that are better suited for limbal epithelial cells, we also confirmed that the proliferative capacity of limbal epithelial cells was markedly decreased, with CFEs comparable to their results, when UV laser power was greater than 50 mW (data not shown). In their study, a laser intensity of 100 mW was used, which can cause significant damage to cells during sorting and may result in diminished proliferative abilities. Additionally, the effects of cultured cells in their study, as opposed to freshly isolated cells, used for FACS in the present case, cannot be excluded. We have, in fact, observed that no SP cells were detected when primary cultured cells were sorted (data not shown), a result that supports our finding that SP cells are growth arrested in vitro.

It has previously been shown that cells that are in active proliferation, such as TA or progenitor cells, but not quiescent adult stem cells, have telomerase activity [28–30]. It is thought that upregulation of telomerase occurs upon differentiation into progenitor or TA cells to prevent the rapid depletion of telomeres during cell division. This process is transient, with telomerase activity decreasing upon the formation of fully differentiated progeny [30]. The corneal epithelium has a relatively short span of renewal, similar to bone marrow, skin, and hair follicles, and therefore the telomerase activity present in the NSP cell fraction likely corresponds to cells that are in active proliferation, such as progenitor or TA cells. Limbal SP cells that have neither telomerase activity nor expression of the differentiated cell markers CK3 and CK12 therefore seem to represent a quiescent stem cell population. NSP cells, which have increased telomerase activity and are clonogenic, likely consist of both TA and progenitor cells that are actively proliferating but not quiescent stem cells, due to both mitotic activity and expression of differentiated CE markers. Finally, CE cells, which express CK3 and CK12, are thought to be highly differentiated cells that express CK3 and CK12, in which telomerase activity has been downregulated because of the loss of proliferative potential.

Our results demonstrate that limbal epithelial SP cells have stem cell–like properties, including growth arrest in the quiescent state, thus meeting the criteria of adult stem cells. It is currently accepted that epithelial stem cells are slow cycling and demonstrate high proliferative potential. However, limbal epithelial SP cells are cell-cycle arrested and, due to their quiescent state, exhibit no in vitro proliferative capabilities. It therefore seems that previously defined epithelial stem cells via colony-forming assays or detection of label-retaining cells may not represent true stem cells, but rather immature progenitor cells. In fact, Oshima et al. [40], discussing their results on adult multipotent stem cells from hair follicles, state that these cells, with high proliferative potential, are likely generated from more immature stem cells.

To accurately identify epithelial stem cells, it seems important to meet the criteria used for other adult stem cells, such as HSCs. The current view is that epithelial stem cells, which demonstrate high proliferative capacity and slow cell cycle, give rise to TA cells, which have a limited number of cell divisions, and finally generate differentiated progeny. We now believe that limbal epithelial SP cells represent an epithelial stem cell population that resides in the quiescent state in the basal layer of the limbus. We also theorize that limbal epithelial SP cells generate progenitor or "active" stem cells that are mitotically cycling and have high proliferative potential. It is these progenitor cells that comprise the portion of the NSP fraction that have active telomerase, demonstrate a slow cell cycle, and have colony-forming abilities. Under normal epithelial cell culture conditions, these colony-forming progenitor cells can proliferate to produce more differentiated cells that can form stratified epithelial layers. CE progenitor cells may therefore be analogous to the multipotent progenitor cells of the hematopoietic system and generate TA cells that are present in the NSP cell fraction of the limbus and can also migrate toward the central cornea to produce the CE cells that express CK3 and CK12. Epithelial stem cells should therefore be defined not by markers of clonogenic or label-retaining cells but by markers of adult stem cells, such

as the SP phenotype via expression of ABCG2; Bmi-1, which regulates stem cell self-renewal; the expression of nestin found in various SP and stem cell populations; and the absence of telomerase activity, representing the cell-cycle arrest of quiescent stem cells.

Previously, we and others have shown the successful clinical transplantation of ex vivo–expanded limbal epithelial cells to human patients [41]. In such cases, the understanding of CE stem cells is of vital importance to the long-term survival of transplanted cells and may contribute to a higher quality of transplantation. However, unlike in the hematopoietic system, where there is an established and accepted in vivo reconstitution assay, the current lack of an analogous model for the corneal epithelial system makes it difficult to confirm the abilities for self-renewal and long-term maintenance of limbal epithelial SP cells. It seems likely, however, that the understanding of the mechanisms that control the proliferation and differentiation of limbal epithelial SP cells will have a significant influence on successful applications in the clinical setting.

ACKNOWLEDGMENTS

We thank Dr. Ai Kushida (Tokyo Women's Medical University) for her technical review and useful comments. This work was supported by Grants-in-Aid for Scientific Research (15390530, 16200036, and 16300161); the High-Tech Research Center Program; the Center of Excellence Program for the 21st Century from the Ministry of Education, Culture, Sports, Science, and Technology in Japan; and the Core Research for Evolution Science and Technology from the Japan Science and Technology Agency.

DISCLOSURES

The authors indicate no potential conflicts of interest.

REFERENCES

1 Arai F, Hirao A, Ohmura M et al. Tie2/angiopoietin-1 signaling regulates hematopoietic stem cell quiescence in the bone marrow niche. Cell 2004;118:149–161.

2 Goodell MA, Brose K, Paradis G et al. Isolation and functional properties of murine hematopoietic stem cells that are replicating in vivo. J Exp Med 1996;183:1797–1806.

3 Zhou S, Schuetz JD, Bunting KD et al. The ABC transporter Bcrp1/ABCG2 is expressed in a wide variety of stem cells and is a molecular determinant of the side-population phenotype. Nat Med 2001;7:1028–1034.

4 Bunting KD. ABC transporters as phenotypic markers and functional regulators of stem cells. STEM CELLS 2002;20:11–20.

5 Kim M, Turnquist H, Jackson J et al. The multidrug resistance transporter ABCG2 (breast cancer resistance protein 1) effluxes Hoechst 33342 and is overexpressed in hematopoietic stem cells. Clin Cancer Res 2002;8:22–28.

6 Scharenberg CW, Harkey MA, Torok-Storb B. The ABCG2 transporter is an efficient Hoechst 33342 efflux pump and is preferentially expressed by immature human hematopoietic progenitors. Blood 2002;99:507–512.

7 Zhou S, Morris JJ, Barnes Y et al. Bcrp1 gene expression is required for normal numbers of side population stem cells in mice, and confers relative protection to mitoxantrone in hematopoietic cells in vivo. Proc Natl Acad Sci U S A 2002;99:12339–12344.

8 Uchida N, Leung FY, Eaves CJ. Liver and marrow of adult mdr-1a/1b(-/-) mice show normal generation, function, and multi-tissue trafficking of primitive hematopoietic cells. Exp Hematol 2002;30:862–869.

9 Shimano K, Satake M, Okaya A et al. Hepatic oval cells have the side population phenotype defined by expression of ATP-binding cassette transporter ABCG2/BCRP1. Am J Pathol 2003;163:3–9.

10 Jackson KA, Mi T, Goodell MA. Hematopoietic potential of stem cells isolated from murine skeletal muscle. Proc Natl Acad Sci U S A 1999;96:14482–14486.

11 Summer R, Kotton DN, Sun X et al. Side population cells and Bcrp1 expression in lung. Am J Physiol Lung Cell Mol Physiol 2003;285:L97–104.

12 Schermer A, Galvin S, Sun TT. Differentiation-related expression of a major 64K corneal keratin in vivo and in culture suggests limbal location of corneal epithelial stem cells. J Cell Biol 1986;103:49–62.

13 Cotsarelis G, Cheng SZ, Dong G et al. Existence of slow-cycling limbal epithelial basal cells that can be preferentially stimulated to proliferate: implications on epithelial stem cells. Cell 1989;57:201–209.

14 Kinoshita S, Friend J, Thoft RA. Sex chromatin of donor corneal epithelium in rabbits. Invest Ophthalmol Vis Sci 1981;21:434–441.

15 Thoft RA, Friend J. The X, Y, Z hypothesis of corneal epithelial maintenance. Invest Ophthalmol Vis Sci 1983;24:1442–1443.

16 Buck RC. Measurement of centripetal migration of normal corneal epithelial cells in the mouse. Invest Ophthalmol Vis Sci 1985;26:1296–1299.

17 Watanabe K, Nishida K, Yamato M et al. Human limbal epithelium contains side population cells expressing the ATP-binding cassette transporter ABCG2. FEBS Lett 2004;565:6–10.

18 Bhattacharya S, Jackson JD, Das AV et al. Direct identification and enrichment of retinal stem cells/progenitors by Hoechst dye efflux assay. Invest Ophthalmol Vis Sci 2003;44:2764–2773.

19 Lechner A, Leech CA, Abraham EJ et al. Nestin-positive progenitor cells derived from adult human pancreatic islets of Langerhans contain side population (SP) cells defined by expression of the ABCG2 (BCRP1) ATP-binding cassette transporter. Biochem Biophys Res Commun 2002;293:670–674.

20 Molofsky AV, Pardal R, Iwashita T et al. Bmi-1 dependence distinguishes neural stem cell self-renewal from progenitor proliferation. Nature 2003;425:962–967.

21 Park IK, Qian D, Kiel M et al. Bmi-1 is required for maintenance of adult self-renewing haematopoietic stem cells. Nature 2003;423:302–305.

22 Raaphorst FM. Self-renewal of hematopoietic and leukemic stem cells: a central role for the Polycomb-group gene Bmi-1. Trends Immunol 2003;24:522–524.

23 Iwama A, Oguro H, Negishi M et al. Enhanced self-renewal of hematopoietic stem cells mediated by the polycomb gene product Bmi-1. Immunity 2004;21:843–851.

24 Zhang P, Iwasaki-Arai J, Iwasaki H et al. Enhancement of hematopoietic stem cell repopulating capacity and self-renewal in the absence of the transcription factor C/EBP alpha. Immunity 2004;21:853–863.

25 Lendahl U, Zimmerman LB, McKay RD. CNS stem cells express a new class of intermediate filament protein. Cell 1990;60:585–595.

26 Chaloin-Dufau C, Sun TT, Dhouailly D. Appearance of the keratin pair K3/K12 during embryonic and adult corneal epithelial differentiation in the chick and in the rabbit. Cell Differ Dev 1990;32:97–108.

27 Wolosin JM, Budak MT, Akinci MA. Ocular surface epithelial and stem cell development. Int J Dev Biol 2004;48:981–991.

28 Ramirez RD, Wright WE, Shay JW et al. Telomerase activity concentrates in the mitotically active segments of human hair follicles. J Invest Dermatol 1997;108:113–117.

29 Bickenbach JR, Vormwald-Dogan V, Bachor C et al. Telomerase is not an epidermal stem cell marker and is downregulated by calcium. J Invest Dermatol 1998;111:1045–1052.

30 Chiu CP, Dragowska W, Kim NW et al. Differential expression of telomerase activity in hematopoietic progenitors from adult human bone marrow. STEM CELLS 1996;14:239–248.

31 Triel C, Vestergaard ME, Bolund L et al. Side population cells in human and mouse epidermis lack stem cell characteristics. Exp Cell Res 2004; 295:79–90.

32 Terunuma A, Jackson KL, Kapoor V et al. Side population keratinocytes resembling bone marrow side population stem cells are distinct from label-retaining keratinocyte stem cells. J Invest Dermatol 2003;121: 1095–1103.

33 Smith KS, Chanda SK, Lingbeek M et al. Bmi-1 regulation of INK4A-ARF is a downstream requirement for transformation of hematopoietic progenitors by E2a-Pbx1. Mol Cell 2003;12:393–400.

34 Milyavsky M, Shats I, Erez N et al. Prolonged culture of telomerase-immortalized human fibroblasts leads to a premalignant phenotype. Cancer Res 2003;63:7147–7157.

35 Moore KA, Lemischka IR. "Tie-ing" down the hematopoietic niche. Cell 2004;118:139–140.

36 Li A, Simmons PJ, Kaur P. Identification and isolation of candidate human keratinocyte stem cells based on cell surface phenotype. Proc Natl Acad Sci U S A 1998;95:3902–3907.

37 Zhu AJ, Haase I, Watt FM. Signaling via beta1 integrins and mitogen-activated protein kinase determines human epidermal stem cell fate in vitro. Proc Natl Acad Sci U S A 1999;96:6728–6733.

38 Jones PH, Watt FM. Separation of human epidermal stem cells from transit amplifying cells on the basis of differences in integrin function and expression. Cell 1993;73:713–724.

39 de Paiva CS, Chen Z, Corrales RM et al. ABCG2 transporter identifies a population of clonogenic human limbal epithelial cells. STEM CELLS 2005;23:63–73.

40 Oshima H, Rochat A, Kedzia C et al. Morphogenesis and renewal of hair follicles from adult multipotent stem cells. Cell 2001;104:233–245.

41 Nishida K, Yamato M, Hayashida Y et al. Functional bioengineered corneal epithelial sheet grafts from corneal stem cells expanded ex vivo on a temperature-responsive cell culture surface. Transplantation 2004; 77:379–385.

A mouse strain difference in tumorigenesis induced by biodegradable polymers

Saifuddin Ahmed, Toshie Tsuchiya
Division of Medical Devices, National Institute of Health Sciences, 1–18-1 Kamiyoga, Setagaya-ku, Tokyo 158-8501, Japan

Received 13 November 2005; accepted 6 February 2006
Published online 00 Month 2006 in Wiley InterScience (www.interscience.wiley.com). DOI: 10.1002/jbm.a.30753

Abstract: The use of poly-L-lactic acid (PLLA) surgical implants for repair of bone fractures has gained popularity in the past decade. The aim of this study was to evaluate the *in vivo* effect of PLLA plates on subcutaneous tissue in two mouse strains, BALB/cJ and SJL/J, which have higher and lower tumorigenicity, respectively. Gap-junctional intercellular communication and protein expression of connexin 43 were significantly suppressed, whereas secretion of transforming growth factor-β1 and expression of extracellular matrix, insulin-like growth factor binding protein 3, and cysteine-rich intestinal protein 2 were significantly increased in PLLA-implanted BALB/cJ mice when compared with BALB/cJ controls. Finally, tumors were formed after implantation of culture cells from the more-tumorigenic BALB/cJ, but not SJL/J, mice into nude mice. © 2006 Wiley Periodicals, Inc. J Biomed Mater Res 78A: 000–000, 2006

Key words: poly-L-lactic acid; gap-junctional intercellular communication; transforming growth factor-β1; connexin 43; nude mice

INTRODUCTION

The morphologic, chemical, and surface electrical characteristics of a biomaterial can influence the extent of the cellular response to an implant,[1,2] but host factors also contribute, so that an identical material implanted in different species[3,4] or at different anatomical locations[5,6] may elicit different degrees of response. Poly-L-lactic acid (PLLA) is a synthetic degradable polymer with good biocompatibility that is widely used clinically for surgical implants and as a bioabsorbable suture material.[7,8] Long-term implants of PLLA produced tumors in rats,[9] and adverse effects were also reported in other animal experiments.[10] All tumors are generally viewed as the result of disruption of the homeostatic regulation of the cell's ability to respond to extracellular signals, which triggers intracellular signal transduction abnormalities.[11] During the transition from the single-cell organism to the multicellular organism, many genes evolved to regulate these cellular functions. One of these genes is the gene coding for a membrane-associated protein channel (the gap junction).[12] Gap-junctional intercellular communication (GJIC) involves two hemichannels or connexons,[13] and each connexon is composed of six basic protein subunits named connexin (Cx), which allow the cell–cell transfer of small molecules. Approximately 20 connexins are known, and they are expressed in a cell- and development-specific manner.[14,15] GJIC also plays an important role in the maintenance of cell homeostasis and in the control of cell growth.[16] Thus, disruption of GJIC has been shown to contribute to the multi-step, multi-mechanism process of carcinogenesis.[17–19] Several tumor-promoting agents have been shown to restrict GJIC by phosphorylation of connexin proteins, such as connexin 43, which is essential in forming the gap junction channel.[20,21] Our previous study revealed that PLLA increased the secretion of transforming growth factor-β1 (TGF-β1), suppressed the mRNA expression of Cx 43, and inhibited GJIC in the early stage after implantation, thus promoting tumorigenesis in BALB/cJ mice.[22] We have hypothesized that the difference in tumorigenic potentials of PLLA is caused mainly by the different tumor-promoting activities of these biomaterials and that TGF-β1 might have an important role in PLLA-implanted BALB/cJ mice. Therefore, in our present experimental approach, we aimed to determine the novel effects of PLLA plates in two mouse strains, BALB/cJ and SJL/J, after long-term implantation. Among mouse strains, the former is a more tumorigenic strain when compared with the latter.[23]

Correspondence to: T. Tsuchiya, e-mail: tsuchiya@nihs.go.jp
Contract grant sponsors: Ministry of Health, Labour and Welfare and Japan Health Sciences Foundation

Immune-deficient nude mice, which are highly susceptible to tumorigenicity, were also used in this experiment.

MATERIALS AND METHODS

Animals

Five-week-old female BALB/cJ and SJL/J, and five-week-old male BALB/cAnCrj-nu mice were purchased from Charles River (Japan) and maintained in the animal center according to the NIHS animal welfare guidelines. All mice were fed standard pellet diets and water *ad libitum* before and after poly-L-lactic acid (PLLA) implantation.

Implantation of PLLA

PLLA was obtained from Shimadzu as uniform sheets. The implants (size, 20 × 10 × 1 mm^3; Mw, 200,000) were sterilized using ethylene oxide gas prior to use. Sodium pentobarbital (4 mg/kg) was intraperitoneally administered to the mice. The dorsal skin was shaved and scrubbed with 70% alcohol. Using an aseptic technique, an incision of ~2 cm was made; a subcutaneous pocket was formed by blunt dissection away from the incision, and one piece of PLLA was placed in the pocket. The incision was closed with silk sutures. In both strains, controls were obtained by sham operation and subsequent subcutaneous pocket formation. Following surgery, the mice were housed in individual cages. After 10 months, mice from the implanted group were killed, implanted materials were excised, and subcutaneous tissues from the adjacent sites were collected for culture. At the same time, subcutaneous tissues were removed from the sites in the sham-operated controls that correlated with the implant sites. Similar experiments were also performed 1 month after PLLA implantation.[22]

Cell culture of subcutaneous tissues

The subcutaneous tissues were maintained in minimum essential medium (MEM) supplemented with 10% FBS in a 5% CO_2 atmosphere at 37°C.

Giemsa staining

When cells reached confluence in tissue culture dishes, they were fixed and stained with Giemsa solution. Cell morphology was determined under an inverted light microscope.

Western blot analysis

When cells had grown confluent in 60-mm tissue culture dishes, all cells were lysed directly in 100 μL 2% sodium dodecyl sulfate (SDS) gel loading buffer (50 m*M* Tris-Hcl, pH 6.8, 100 m*M* 2-mercaptoethanol, 2% SDS, 0.1% bromophenol blue, and 10% glycerol). The protein concentration of the cleared lysate was measured using a micro-plate BCA protein assay (Pierce, Rockford, IL). Equivalent protein samples were analyzed by 7.5% SDS-polyacrylamide gel electrophoresis. The proteins were transferred to Hybond-ECL nitrocellulose membranes (Amersham Pharmacia Biotech UK, Buckinghamshire, UK), and Cx 43 protein was detected by anti-Cx 43 polyclonal antibodies (ZYMED Laboratories, San Francisco, CA). The membrane was soaked with Block Ace (Yukijirushi Nyugyo, Sapporo, Japan), reacted with the anti-Cx 43 polyclonal antibodies for 1 h, and after washes with PBS containing 0.1% Tween20, reacted with the secondary anti-rabbit IgG antibody conjugated with horseradish peroxidase for 1 h. After several washes with PBS-Tween20, the membrane was detected with the ECL detection system (Amersham Pharmacia Biotech UK).

Scrape-loading and dye transfer assay

The scrape-loading and dye transfer (SLDT) technique was performed by the method of El-Fouly et al.[24] Confluent monolayer cells in 35-mm culture dishes were used. After rinsing with Ca^{2+}, Mg^{2+} phosphate-buffered saline [PBS(+)], cell dishes were loaded with 0.1% Lucifer Yellow (Molecular Probes, Eugene, OR) in PBS(+) solution and were scraped immediately with a sharp blade. After incubation for 5 min at 37°C, cells were washed three times with PBS(+), and the extent of dye transfer was monitored using a fluorescence microscope equipped with a type UFX-DXII CCD camera and a super high-pressure mercury lamp power supply (Nikon, Tokyo, Japan).

Enzyme-linked immunosorbent assay

Cells were seeded onto 60-mm dishes. The conditioned medium was collected after centrifugation at 1000 rpm for 2 min. The transforming growth factor-β1 (TGF-β1) levels of the media were measured with commercially available enzyme linked immunosorbent assay (ELISA) kits (R&D Systems, Minneapolis, MN).

DNA microarray analysis

At least 10^7 cells were harvested and frozen in liquid nitrogen. Total RNA was extracted, purified, and assessed for yield and purity, and cDNA probes were synthesized with the Atlas™ Pure Total RNA Labeling System (Clontech) according to the manufacturer's instructions. Hybridization of the ^{33}P-labeled probes to the Atlas Array of Mouse

Cancer 1.2 k Array (Clontec 7858–1), on which 1176 cDNAs of cancer-related genes were spotted, was performed with Atlas™ cDNA Expression Arrays according to the manufacturer's instructions. The phosphor images of hybridized arrays were analyzed with AtlasImage™ (Clontech). Genes that were up- or downregulated more than fivefold relative to the negative controls are discussed.

Determination of tumorigenicity in nude mice

Cultured cells were harvested by trypsinization, and 2×10^6 washed cells suspended in 0.2 mL of PBS were inoculated at a single subcutaneous site into 6–8-week-old nude mice. All mice were examined regularly for the development of tumor.

Soft agar assay

Approximately 100,000 cells per well from each clone were seeded in 2 mL of 0.3% soft agar in culture medium on a solidified basal layer in 6-well tissue culture plates. The plates were cultured for 4 weeks and then stained with *p*-iodotetrazolium violet for 48 h before counting.

Statistical analysis

Student *t* tests were used to assess whether differences observed between the implanted and control samples were statically significant. For comparison of groups of means, one-way analysis of variance was carried out. When significant differences were found, Tukey's pairwise comparisons were used to investigate the nature of the difference. The confidence level was set at 95% for all tests. Statistical significance was accepted at $p < 0.05$. Values were presented as the mean ± SD.

RESULTS

Giemsa staining

Cells with different morphologies formed a slightly crisscrossed pattern in the BALB/cJ control group, whereas cells in the implanted groups of BALB/cJ showed a markedly crisscrossed pattern. The cells were extensively piled up, which decreased contact inhibition, under inverted light microscopy observation and Giemsa staining [Fig. 1(A,B)]. In contrast, the cells of the SJL/J group formed a parallel, flat, confluent monolayer that maintained contact inhibition [Fig. 1(C,D)].

Western blot analysis

We examined the protein expression of the connexin 43 gene and found that the total protein level was significantly decreased in PLLA-implanted BALB/cJ mice when compared with that in BALB/cJ controls (Fig. 2). However, protein expression was decreased in both control and PLLA-implanted groups in SJL/J mice (Fig. 2). F2

SLDT assay

The SLDT assay was used to assess functional gap-junctional intercellular communication (GJIC). GJIC was significantly inhibited in PLLA-implanted BALB/cJ mice when compared with that in BALB/cJ controls (Fig. 3). A significant difference was also observed between the two strains of mice in that the GJIC was lower in SJL/J than in BALB/cJ group (Fig. 3). F3

ELISA

The secretion of TGF-β1 was significantly increased in PLLA-implanted BALB/cJ subcutaneous tissues in comparison with that from BALB/cJ control mice. On the contrary, secretion of TGF-β1 tended to decrease in the SJL/J implanted mice when compared with that in SJL/J control mice (Fig. 4). F4

DNA microarray analysis of the four kinds of cells

Expression of the major ECM [fibronectin 1, procollagen VIIIα 1, and osteopontin precursor (OPN)] proteins [Fig. 5(A–C)], insulin-like growth factor binding protein (IGFBP) 3 [Fig. 5(D)], and cysteine-rich intestinal protein 2 (CRIP 2) [Fig. 5(E)] were increased in the PLLA-implanted BALB/cJ mouse cells when compared with that in BALB/cJ control mouse cells. No such difference was observed between SJL/J implanted and control mouse cells. F5

Tumorigenicity in nude mice

No tumor was formed in PBS(−) injected nude mice [Fig. 6(A)]. Rapid growth of large tumors was observed in nude mice within 2 weeks of injection of cultured cells from PLLA-implanted BALB/cJ mice [Fig. 6(B,C,E,F)]. Nude mice injected with HeLa cells, which served as positive controls, showed slower F6

tapraid5/za1-jbmmain/za1-jbmmain/za101006/za11353d06a | royerl | S=4 | 4/26/06 | 5:41 | Art: 30753 | Input-bp

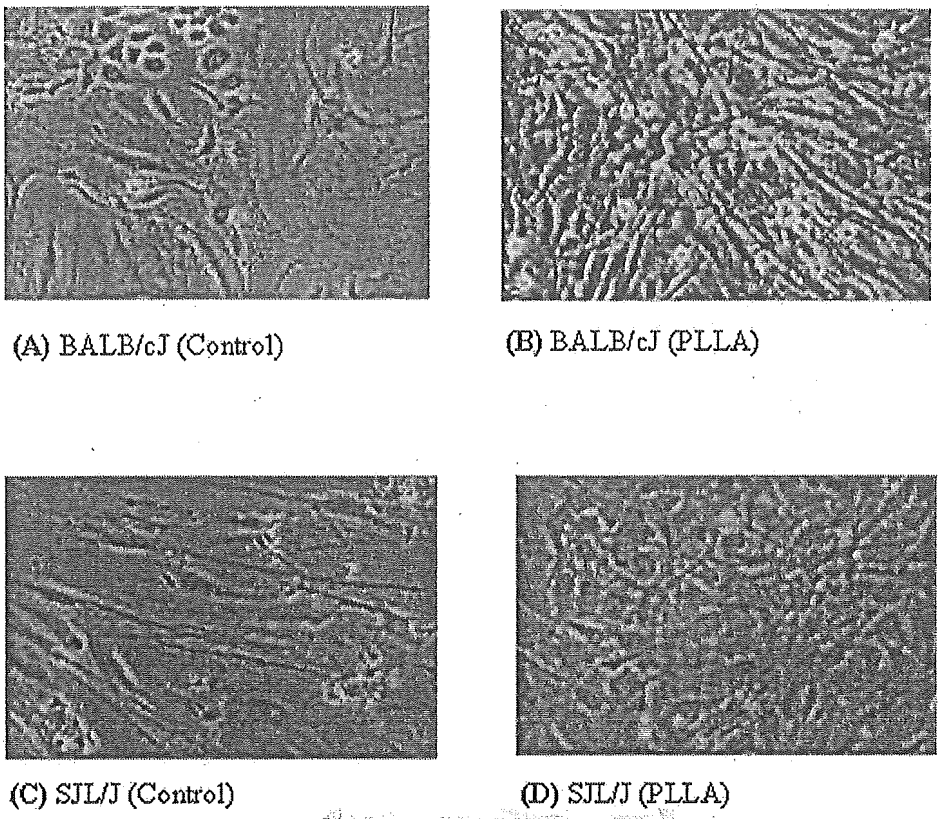

Figure 1. Mouse cell morphology. Three each of both implanted mice and sham-operated controls were killed after 10 months. Results shown are representative of two independent experiments. Inverted light microscopic appearance (magnification ×100) of (A) BALB/cJ (control), (B) BALB/cJ (PLLA), (C) SJL/J (control), and (D) SJL/J (PLLA). [Color figure can be viewed in the online issue, which is available at www.interscience.wiley.com.]

AQ: 1

growth of tumor 4 weeks after cell injection [Fig. 6(D,G)].

Soft agar assay

These tumor cells did not form a colony in soft agar (data not shown), although HeLa cells did form colonies in soft agar.

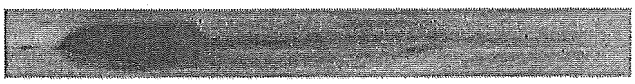

Figure 2. Expression of Cx 43 protein by Western blot analysis. Three each of both implanted mice and sham-operated controls were killed after 10 months. Results shown are representative of two independent experiments. Total protein expression significantly decreased in PLLA-implanted BALB/cJ mice when compared with that in the control. However, protein expression decreased in both control and PLLA-implanted groups in SJL/J mice.

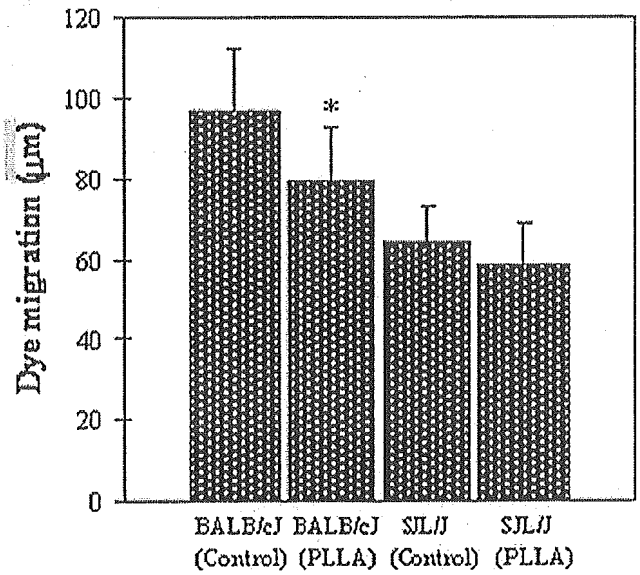

Figure 3. Statistical analysis of SLDT assay. Three each of both implanted mice and sham-operated controls were killed after 10 months. Results shown are representative of two independent experiments. GJIC was found to be significantly inhibited in PLLA-implanted BALB/cJ mice cells when compared with that in BALB/cJ controls. *$p < 0.05$.